Milling Force Analysis of SiCp/Al Complex Thin-Walled Parts Based on Finite Element Method

Kai Xu and Niansong Zhang
College of Mechanical Engineering, Nanjing University of Science and Technology, Nanjing, China
Email: 736163891@qq.com,zns@ustc.edu.cn

Aimin Wang
College of Mechanical Engineering, Beijing Institute of Technology, Beijing, China
Email: wangam@bit.edu.cn

***Abstract*—The difficulty of machining deformation control of a SiCp/Al complex thin-walled part is described. The theoretical analysis and simulation pretreatment modeling of SiCp/Al composite hard and brittle materials were carried out. A constitutive model of SiCp/Al composite hard and brittle materials was established. The milling force in the actual machining process was simulated by the finite element method, and the influence of each machining parameter on the milling force of thin-walled parts was analyzed. Set up multiple sets of control experiments to get the best processing parameters.**

***Index Terms*—Si Cp/Al, thin-walled parts, finite element simulation, deformation control**

I. Introduction

In the numerical control machining process of large-scale thin-walled monolithic structural parts, machining deformation has become a common problem in the field of processing and manufacturing. The deformation after CNC machining not only affects normal assembly, but also has a great negative impact on the performance and quality of components.

In this paper, for the SiCp/Al complex thin-walled parts, the most prone to deformation in the 11-step machining process is to finish the large plane to the size, and ensure that the parallelism of the top and bottom end faces is 0.05. This report uses finite element simulation. Analytical techniques to study the influence of the processing parameters of large thin-walled parts on the milling force in the process of milling large planes, through multiple sets of control groups to compare and analyze, to determine the processing parameters of this process.

II. Theoretical Analysis of SiCp/Al Composite Hard and Brittle Materials

The aluminum-based silicon carbide material is not a homogeneous material, but a silicon carbide particle having a diameter of a micron order is dispersed in the metal aluminum-based phase [1]. The aluminum-based silicon carbide material can be regarded as a plurality of micro-body units arranged in a certain period, and each individual unit is composed of one SiC particle and an aluminum base surrounding the same [2]. Although aluminum-based silicon carbide is homogeneous in macroscopic view, microscopically, when the volume fraction of SiCp/Al material and the diameter of SiC particles change, it will have a huge impact on the macroscopic properties of the material. Based on the homogenization theory and Mori-Tanaka mean field theory, this paper calculates the macroscopic properties of heterogeneous aluminum-based silicon carbide materials and calculates the equivalent elastic modulus of different volume fractions of SiCp/Al by theoretical calculation.

After the aluminum-based silicon carbide material is processed by high temperature and high pressure, the bonding surface of the SiC particle reinforcing phase and the Al-based phase is strengthened, and the macroscopic properties of the material are further enhanced. However, the arrangement of the strengthening layer is disorderly, and it is difficult to measure the thickness. In view of this situation, according to the Mori-Tanaka rule, the strengthening layer needs to be equivalent to the boundary layer without thickness, and the deformation of the strengthening layer itself simplifies the transaction. Displacement at both ends of the layer

The stress and strain of the SiC particles are set to $\overline{\sigma_{ij}^{r}}$, $\overline{\varepsilon_{ij}^{r}}$, The stress and strain of the Al matrix are $\overline{\sigma_{ij}^{m}}$, $\overline{\varepsilon_{ij}^{m}}$, Then the stress of SiCp/Al $\overline{\sigma_{ij}}$ and strain $\overline{\varepsilon_{ij}}$ can be expressed as [3]:

Manuscript received August 1, 2019; revised April 1, 2020.

doi: 10.18178/ijmerr.9.5.685-690

$$\begin{cases} \overline{\sigma_{ij}} = f\overline{\sigma_{ij}^{r}} + (1-f)\overline{\sigma_{ij}^{m}} \\ \overline{\varepsilon_{ij}} = f\overline{\varepsilon_{ij}^{r}} + (1-f)\overline{\varepsilon_{ij}^{m}} + \dfrac{1}{2V}\int_{s}([u_i]n_j + [u_j]n_i)ds \end{cases} \quad (1)$$

At the same time, the equivalent elastic modulus $\overline{C_{ijkl}}$ should be satisfied [4]:

$$\overline{\sigma_{ij}} = \overline{\varepsilon_{kl}}\,\overline{C_{ijkl}} \quad (2)$$

When the aluminum-based silicon carbide material has uniform strain ε_{ij}^{0}, it is assumed that the strain of the silicon carbide particles is $\overline{\varepsilon_{ij}^{r}} = T\varepsilon_{kl}^{0}$, $[u_i] = \psi_{ikl}\varepsilon_{kl}^{0}$ at this time, and the elastic modulus tensor of the Al matrix and the silicon carbide particles are C_{ijkl}^{m}、C_{ijkl}^{r} respectively . From equations (1) and (2), the equivalent modulus of aluminum-based silicon carbide can be expressed as:

$$\overline{C_{ijkl}} = C_{ijpq}^{m}\left[I_{pqkl} + f\left(D_{ijpq}^{m}C_{pqst}^{r} - I_{ijst}\right)T_{stkl} - \frac{1}{2V_r}\int_{V_t}\left(\psi_{ikl,\,j} + \psi_{jkl,\,i}\right)dV\right] \quad (3)$$

Based on the Mori-Tanaka theory, considering the strengthening effect of the bonding surface between the aluminum-based phase and the silicon carbide particles, the elastic modulus calculation model of the silicon carbide particle reinforcing material is established. It is assumed that stress $\overline{\sigma_{ij}^{m}}$ and strain $\overline{\varepsilon_{ij}^{m}}$ are uniformly applied to the silicon carbide particles of the strengthening layer on the infinite aluminum base phase. According to the elastic solution of the inclusion particles by Meguid.S.A, the average stress $\overline{\sigma_{ij}^{r}}$ and average strain $\overline{\varepsilon_{ij}^{r}}$ of the silicon carbide particles can be determined as:

$$\overline{\sigma_{ij}^{r}} = \Lambda_{ijkl}^{\sigma}\,\overline{\sigma_{kl}^{m}} \quad (4)$$

$$\overline{\varepsilon_{ij}^{r}} = \Lambda_{ijkl}^{\varepsilon}\,\overline{\varepsilon_{kl}^{m}} \quad (5)$$

The Λ_{ijkl}^{σ} and $\Lambda_{ijkl}^{\varepsilon}$ in the sum in the formulas (4) and (5) can be expressed as:

$$\begin{cases} \Lambda_{ijkl}^{\sigma} = \dfrac{\Lambda_1^{\sigma}}{3}\delta_{ij}\delta_{kl} + \dfrac{\Lambda_1^{\sigma}}{2}\left[\delta_{ik}\delta_{jl} + \delta_{il}\delta_{jk} - \dfrac{2}{3}\delta_{ij}\delta_{kl}\right] \\ \Lambda_{ijkl}^{\varepsilon} = \dfrac{\Lambda_1^{\varepsilon}}{3}\delta_{ij}\delta_{kl} + \dfrac{\Lambda_1^{\varepsilon}}{2}\left[\delta_{ik}\delta_{jl} + \delta_{il}\delta_{jk} - \dfrac{2}{3}\delta_{ij}\delta_{kl}\right] \end{cases} \quad (6)$$

The Λ_1^{ε}、Λ_2^{ε}、Λ_1^{σ} and Λ_2^{σ} can be expressed as :

$$\Lambda_1^{\varepsilon} = 1 + \frac{1+v}{3(1-v)}\lambda_1 + \frac{2(1-2v)}{3(1-v)}\lambda_2 \quad (7)$$

$$\Lambda_2^{\varepsilon} = 1 + \frac{2(4-5v)}{15(1-v)}\left[M_1 + \frac{2}{5}N_1 + \frac{3}{5}S_1\right] + \frac{7-5v}{15(1-v)}\left[P_1 + \frac{2}{5}Q_1\right] \quad (8)$$

$$\Lambda_1^{\sigma} = 1 - \frac{2(1-2v)}{3(1-v)}(\lambda_1 - \lambda_2) \quad (9)$$

$$\Lambda_2^{\sigma} = 1 - \frac{7-5v}{15(1-v)}\left[M_1 + \frac{2}{5}N_1 + \frac{3}{5}S_1 - P_1 - \frac{2}{5}Q_1\right] \quad (10)$$

where λ_1、λ_2、M_1、N_1、P_1 and Q_1 have been found in the M-T formula, v is the Poisson's ratio of the aluminum-based silicon carbide material, and the combined stress (tensor) and tensor of the silicon carbide particles can be derived by combining (1):

$$T_{ijkl} = \Lambda_{ijmn}^{\varepsilon}t_{mnkl}^{-1} \quad (11)$$

$$R_{ijkl} = \Lambda_{ijmn}^{\sigma}r_{mnkl}^{-1} \quad (12)$$

$$t_{mnkl} = (1-f)I_{mnkl} + f\left(\Lambda_{ijkl}^{\varepsilon} + j_{ijkl}\right) \quad (13)$$

$$r_{mnkl} = (1-f)I_{ijkl} + f\Lambda_{ijkl}^{\sigma} \quad (14)$$

The displacement partition on both sides of the bonding layer between the silicon carbide particles and the aluminum base is known from the following formula:

$$[u_i] = \left[\frac{1}{3}(P_1 + Q_1 - \lambda_2)\delta_{mn}x_i - P_1\delta_m x_n - \frac{Q_1}{\alpha^2}x_i x_m x_n\right]t_{mnkl}^{-1}\varepsilon_{kl}^{0} \quad (15)$$

According to the formulas (3) and (5), when a uniform strain is applied at infinity, the bulk modulus of the aluminum matrix, the silicon carbide particles, and the aluminum-based silicon carbide material has the following relationship:

$$\frac{\overline{K}}{K^{m}} = \frac{1 - f + f\Lambda_1^{\varepsilon}\dfrac{K^{r}}{K^{m}}}{1 - f + f\left(\Lambda_1^{\varepsilon} - \lambda_2\right)} \quad (16)$$

According to the classical formula [5]:

$$E = 3K(1-2u) \quad (17)$$

This study studies the body fraction of SiCp/Al is f=45%, Poisson's ratio is u=0.25. According to the above formula, the equivalent elastic modulus can be calculated E=157Gpa.

The whole milling process has problems such as large strain, high strain rate and large temperature change. Only by establishing the constitutive model of the material and understanding the relationship between the stress at the large strain rate and the temperature and strain rate, the material can be milled. The elastoplastic deformation law in the simulation process is accurately expressed. The constitutive model of the material is generally expressed by its

function of temperature, strain and strain rate. The constitutive models of the commonly used thermo-elastic (viscous) plastic materials are: Power-Law model, Johnson-Cook model. , Litonski-Batra model and Bodner-Partom model. Compared with several other models, the Johnson-Cook model not only considers factors such as strain, strain rate and thermal softening, but also involves few parameters and is easy to obtain, and can adapt to different kinds of materials. This model is used in this section when using AdvantEdge software simulation. The mathematical expression of the model is:

$$\sigma = \left(A + B\varepsilon^{P}\right)\left[1 + C\ln\left(1 + \frac{\varepsilon}{\varepsilon_0}\right)\right]\left(1 - \theta_T^{*\mathrm{m}}\right) \tag{18}$$

$$\theta_T^{*\mathrm{m}} = \frac{\theta - \theta_{\mathrm{r}}}{\theta_{\mathrm{m}} - \theta_{\mathrm{r}}} \tag{19}$$

A=982Mpa, B=643.467Mpa, C=0.015, m=1.223, P=0.227.

III. Finite Element Simulation Results and Data Processing

A. Introduction to Finite Element Simulation

Finite element analysis (FEA, Finite Element Analysis) uses mathematical approximation to simulate real physical systems (geometry and load cases). With simple and interacting elements (ie, units), a finite number of unknowns can be used to approximate an infinitely unknown real system [6].

The finite element method was originally called the matrix approximation method, applied to the structural strength calculation of aircraft, and attracted the interest of scientists engaged in mechanics research due to its convenience, practicability and effectiveness [7]. After a few decades of hard work, with the rapid development and popularization of computer technology, the finite element method has rapidly expanded from structural engineering strength analysis and calculation to almost all fields of science and technology, becoming a colorful, widely used, practical and efficient Numerical analysis method.

The commonly used finite element analysis softwares include ABAQUS, ANSYS, LS-DYNA, AdvantEdge FEM, DEFORM, etc [8]. In this experiment, AdvantEdge FEM software suitable for machining simulation is selected.

B. Milling Force Theory Modeling

1) Three-dimensional force model of Won-Soo Yun

The cutting force model of the model is as follows:

$$F_x(j) = \sum_k \sum_i F_x(i, j, k) \tag{20}$$

$$F_{\mathrm{y}}(j) = \sum_k \sum_i F_y(i, j, k) \tag{21}$$

$$F_{\mathrm{z}}(j) = \sum_k \sum_i F_z(i, j, k) \tag{22}$$

Among them $F_{\mathrm{x}}(\mathrm{i,j,k})$、$F_{\mathrm{y}}(\mathrm{i,j,k})$、$F_{\mathrm{z}}(\mathrm{i,j,k})$ are thr force representing the three directions of the microcell, respectively, whose expression is:

$$F_x(i, j, k) = \left(C_1 K_n \cos(\eta - \alpha_r) + K_f K_n C_3 \cos\eta - K_f K_n C_4 \sin(\eta - \alpha_r)\right) t_c(\eta) B_1 \tag{23}$$

$$F_{\mathrm{y}}(i, j, k) = \left(C_1 K_n \sin(\eta - \alpha_r) + K_f K_n C_3 \cos\eta - K_f K_n C_4 \cos(\eta - \alpha_r)\right) t_c(\eta) B_1 \tag{24}$$

$$F_{\mathrm{z}}(i, j, k) = \left(-C_2 K_n + K_f K_n C_5\right) t_c(\eta) B_1 \tag{25}$$

2) Mechanical model based on empirical formula

The milling force model established by Wang Litao and others to study the machining deformation of aerospace aluminum alloys uses the multi-factor regression orthogonal experiment method for milling experiments. Based on the four-factor and four-level experimental models, the constant coefficients and exponential mathematical derivation formulas are given. The expression of the main milling force is presented as:

$$F_z = C_F \alpha_e^{0.86} \alpha_f^{0.72} d^{-0.83} \alpha_p Z \tag{26}$$

Some people in China have also given the formula of the main milling force when machining high-speed steel end mills for gray cast iron and carbide end mills for carbon steel.

$$F_{\mathrm{c}} = 9.81 \alpha_e^{0.83} f_z^{0.65} d_0^{-0.83} \alpha_p Z \tag{27}$$

$$F_{\mathrm{c}} = 9.81 \alpha_e^{1.1} f_z^{0.75} \mathrm{n}^{-0.2} d_0^{-1.3} \alpha_p Z \tag{28}$$

It can be seen from the above formula that although the processing object and the environmental factors are different, the milling force is basically constructed in the same form, but the contribution factors of the parameters that are inconsistent in the speed parameter or the parameters of the experimenter are different.

At the same time, the speed parameter in the milling process can not be ignored. On the one hand, the milling speed determines the frequency of the cutting and cutting of the workpiece, which affects the fluctuation law of the milling force. On the other hand, the milling speed improves the cutting effect during the machining process. The effect, especially in high-speed milling, is particularly effective. Therefore, the formation of the milling force model is determined as:

$$F_\theta = C_{F_\theta} \cdot \alpha_P^{X_{F\theta}} \cdot V^{Y_{F\theta}} \cdot \alpha_W^{\mathrm{n}_{F\theta}} \cdot d \cdot Z \tag{29}$$

C. Finite Element Simulation Process

Four sets of control test groups were set up, the fixed feed rate = 0.1 mm/tooth, the depth of cut = 0.2 mm, the cut width = 6 mm, and the rotational speeds were 500 r/min and 525 r/min, respectively. , 550r/min, 575r/min. Obtain the results shown in Fig. 1 (a), (b), (c), (d).

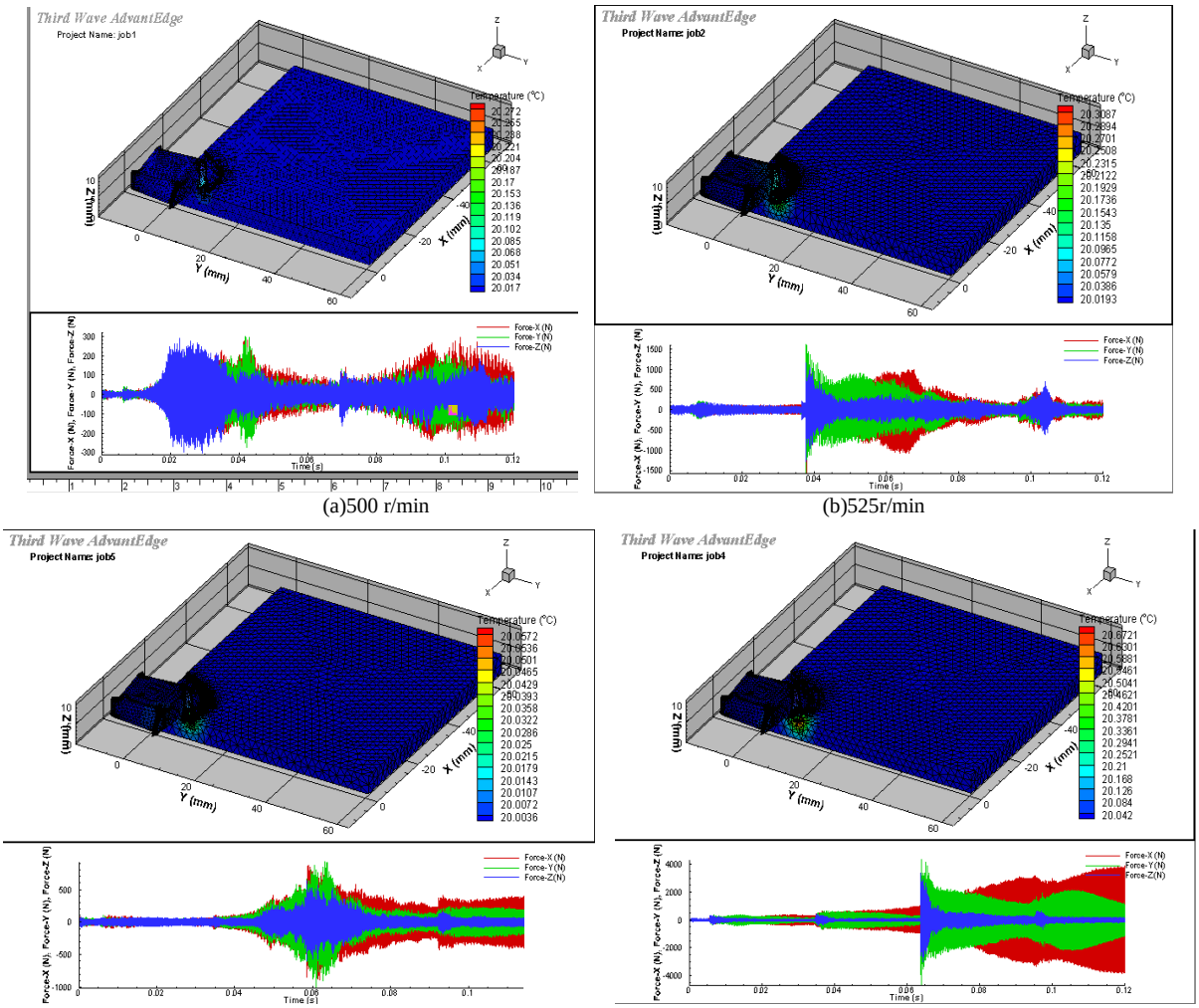

(a)500 r/min (b)525r/min

(c)550r/min (d)575r/min

Figure 1. Simulation results of relationship between rotational speed and axial force.

When the tool is cut into the work-piece, the load in the axial direction is not very large, and the cutting force in the X and Y directions is relatively large. After cutting into a process, the tool is subjected to the cutting process. The axial cutting force is gradually increased.

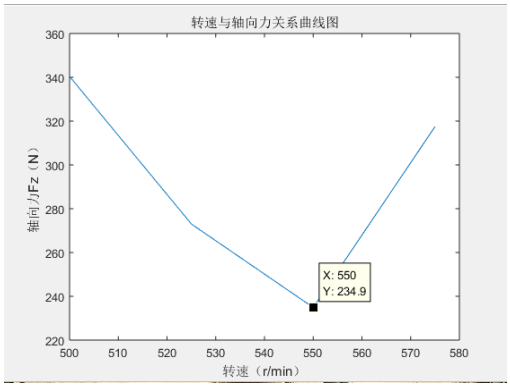

Figure 2. Speed and axial force curve.

Plot the relationship between the rotational speed and the axial force in Fig. 2 in Matlab.

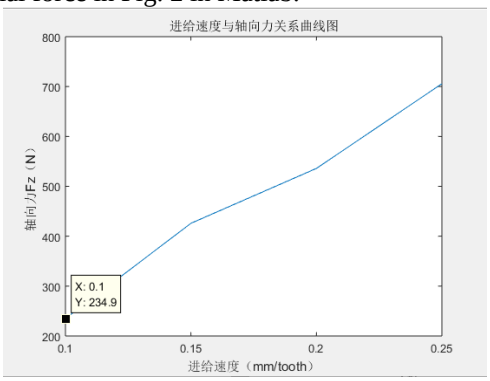

Figure 3. Feed speed and axial force curve.

Axial force changes firstly and then increases when the rotational speed is in the range of 500-575 r/min. The axial force takes the minimum value of 234.9 N when the rotational speed reaches 550 r/min. This shows that when

milling the large plane of SiCp/Al workpiece, the rotation speed is not as high as possible.

Fixed speed = 550r/min, depth of cut = 0.2mm, width of cut = 6mm, feed rate was 0.1mm/tooth, 0.15 Mm/tooth, 0.20mm/tooth, 0.25mm/tooth. Obtain the graph of the relationship between the rotational speed and the axial force in Fig. 3.

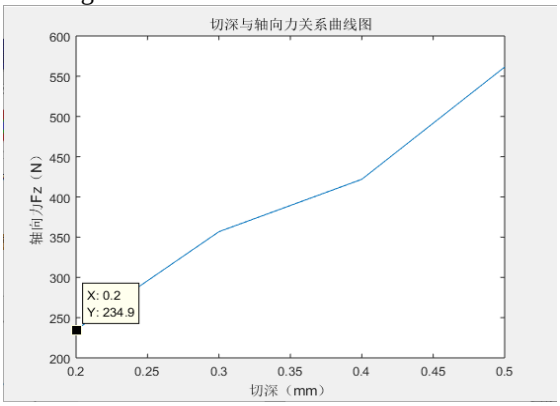

Figure 4. Cut depth and axial force curve.

Feed rate has a great influence on the axial force cutting force generated when milling the SiCp/Al work-piece. In the range of 0.1mm/tooth to 0.25mm/tooth, the work-piece increases with the feed rate. The axial force Fz is linearly rising, so a small feed rate should be used in the actual machining process.

Four sets of control test groups were set up, fixed speed = 550r/min, feed rate = 0.1mm/tooth, cut width = 6mm, depth of cut was 0.2mm, 0.3 Mm, 0.4mm, 0.5mm. Obtain the graph of the relationship between the depth of cut and the axial force as shown in Fig. 4.

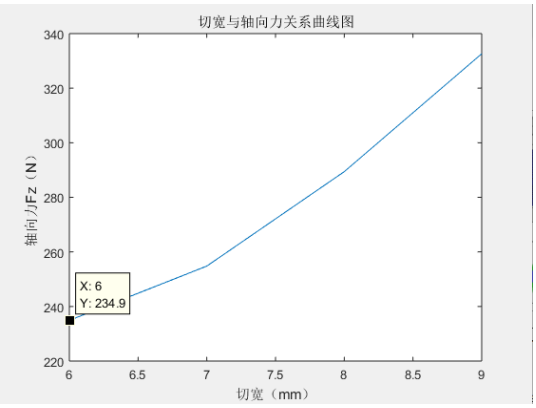

Figure 5. Cut width and axial force curve.

As the depth of cut increases, the axial force increases linearly. It shows that the depth of cut has a great influence on the milling deformation.

Four sets of control test groups were set up, fixed speed = 550r/min, feed rate = 0.1mm/tooth, depth of cut = 0.2mm, and width of cut was 6mm, 7mm respectively. , 8mm, 9mm. Obtain the graph of the relationship between the width and the axial force.

From the above figure, the effect of the width of the cut on the axial force is not affected by the rotational speed, the feed rate and the depth of cut. This may be because the cutting width mainly affects the radial force and the axial force.

IV. Conclusion

The above milling force is reloaded onto the part by ANSYS to simulate the deformation during actual machining, as shown in the Fig. 6.

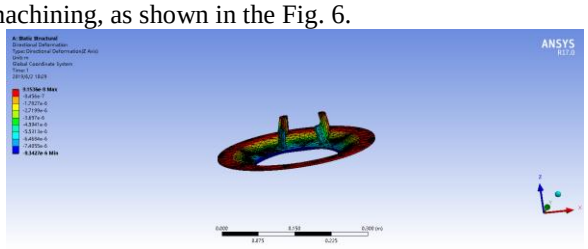

Figure 6. Reloading the milling force in ANSYS to obtain the deformation cloud.

The deformation amount after reloading of all the above simulation groups is as shown in Table I.

TABLE I. Deformation under Each Processing Parameter

Serial number	Rotating speed (r/min)	Feed rate (mm/tooth)	Cutting width (mm)	Cut depth (mm)	Deformation maximum deformation (mm)
1	500	0.1	0.2	6	0.12075
2	525	0.1	0.2	6	0.024893
3	550	0.1	0.2	6	0.0183427
4	575	0.1	0.2	6	0.097627
5	550	0.15	0.2	6	0.247535
6	550	0.2	0.2	6	0.278542
7	550	0.25	0.2	6	0.387459
8	550	0.1	0.3	6	0.194752
9	550	0.1	0.4	6	0.261247
10	550	0.1	0.5	6	0.324775
11	550	0.1	0.2	7	0.012435
12	550	0.1	0.2	8	0.016475
13	550	0.1	0.2	9	0.022758

Comparing the deformation amount in the above table with the processing flatness requirement of the part of 0.05, it is possible to select a set of processing parameters with higher processing efficiency under the premise of ensuring the machining accuracy. The actual machining and simulation results will have some errors, and it is necessary to set aside certain. The remaining amount of processing, so the optimal processing parameters that can be selected are 550r/min, feed rate of 0.1mm/tooth, depth of cut of 0.2mm, and width of cut of 9mm.

Conflict of Interest

The authors declare no conflict of interest.

Author Contributions

Niansong Zhang conducted the research; Aimin Wang analyzed the data; Kai Xu wrote the paper.

References

[1] J. C. Shao, B. L. Xiao, Q. Z. Wang, Z. Y. Ma, K. Yang, "An enhanced FEM model for particle size dependent flow strengthening and interface damage in particle reinforced.metal

matrix composites," *Composites Science and Technology*, vol. 71, pp. 39-45, 2011.
[2] J. Segurado, J. LLorca, "A new three-dimensional interface finite element to simulate fracture in composites," *International Journal of Solids and Structures*, vol. 41, pp. 2977-2993, 2004.
[3] C. R. Dandekar, Y. C. Shin, "Multiphase finite element modeling of machining unidirectional composites: Prediction of debonding and fiber damage," *Manuf Sci Eng,Trans ASME* , vol. 130, pp. 1-12, 2008.
[4] A. Pramanik, L. C. Zhang, "Micro-indentation of metal matrix composites-an FEM analysis," *Key Eng Mater*, vol. 340-341, pp. 563-570, 2007.
[5] C. R. Dandekar, Y. C. Shin, "Multi-step 3-D finite element modeling of subsurface damage in machining particulate reinforced metal matrix composites," *Composites: Part A*.. vol. 40, pp. 1231-1239, 2009.
[6] Y. B. Guo, "An intergral method to determine the mechanical behabior of materials in metal cutting," *J. Journal of Materials Processing Techology*, vol. 142, pp.72-81, 2003.
[7] Y. L. Li, K. T. Ramesh, E. S. C. Chin, "The mechanical response of an A359/Si Cp MMC and the A359 aluminum matrix to dynamic shearing deformations," *Materials Science and Engineering A*, vol. 382, pp. 162-170, 2004.
[8] K. Carlsson, "Modeling of three dimensional microstructures including grain boundary mechanisms," Master's thesis 2013:51.

Kai Xu is with the College of Mechanical Engineering, Nanjing University of Science and Technology, Nanjing, China. He has received the bachelor of mechanical engineering's degree and the master of mechanical engineering's degree.

Niansong Zhang is with the College of Mechanical Engineering, Nanjing University of Science and Technology, Nanjing, China. In July 2006, he graduated from the Department of Precision Instruments and Mechanics of Tsinghua University with a doctorate in engineering. He was hired as the Jiangsu Provincial Science and Technology Commission from 2012 to 2015, teaching doctoral talents to enter the enterprise talents.

Aimin Wang is with the College of Mechanical Engineering, Beijing Institute of Technology, Beijing, China. In 2003.1-2005.3, he was stayed in Tsinghua University, National CIMS Engineering Technology Research Center, engaged in post-doctoral research work in the field of control science and engineering. After that, he is staying in Beijing Institute of Technology, Department of Manufacturing Engineering, School of Mechanical and Vehicle Engineering, Digital Manufacturing Research Institute, work till now.